

Effect of small floating disks on the propagation of gravity waves

F. De Santi^{1,2} & P. Olla^{1,2†}

¹ISAC-CNR, Sez. Cagliari, I-09042 Monserrato, Italy

²INFN, Sez. Cagliari, I-09042 Monserrato, Italy

(Received xx; revised xx; accepted xx)

A dispersion relation for gravity waves in water covered by disk-like impurities floating in a viscous matrix is derived. The macroscopic equations are obtained ensemble-averaging the fluid equations at the disk scale in the asymptotic limit of long waves and low disk surface fraction. Various regimes have been identified depending on the disk radii and the thickness and viscosity of the top layer. Semi-quantitative analysis in the close-packing regime suggests dramatic modification of the dynamics, with order of magnitude increase in wave damping and wave dispersion. Possible relevance of the results to wave propagation in ice-covered ocean is discussed, and comparison with field data is provided.

Key words: surface gravity waves, complex fluids, sea ice.

1. Introduction

Materials floating on the surface of the ocean affect the propagation of gravity waves: oil slicks have long been known to produce wave attenuation; similar effects are produced by grease ice, is the ice crystal suspension constituting one of the first phases of formation of sea-ice; larger objects, such as floating debris, wave-breaking buoys, ice floes, will have a more complicated effect, but attenuation is usually dominant.

Such issues are of great interest in sea ice dynamics and may find application in oil spill detection (Brekke & Solberg 2005). Gravity waves play an important role in sea ice formation (Martin & Kauffman 1981; Dai et Al. 2004) and destruction through floes break-up (Kohout & Meylan 2008). Remote sensing of wave propagation could be used to determine the thickness of the ice cover in polar seas (Wadhams et Al. 2002, 2004), which is a problem of great relevance in the study of climate change.

Over the years, several models of wave propagation in ice covered waters have been proposed (Squire et Al. 1995). Weber (1987) treated grease ice as a very viscous medium in creeping flow conditions. Keller (1998) extended the model to generic values of the viscosity. Various generalizations have been proposed to include the effect of an eddy viscosity in the otherwise inviscid bottom region (De Carolis & Desiderio 2002), the possibility of a viscoelastic component in the ice (Wang & Shen 2010), spatial inhomogeneities (Wang & Shen 2011). Attempts to derive the rheology of grease ice from the microscopic dynamics of the ice crystal have also been proposed (De Carolis et Al. 2005).

Extension of such models to conditions in which the first solid ice begins to form—the so called pancake ice, which is an agglomerate of disk-shaped ice blocks (the pancakes) floating on a grease ice layer of more or less the same depth—have given mixed results (Wadhams et Al. 2004; Wang & Shen 2010).

† Email address for correspondence: olla@dsf.unica.it

In the case of large floes, the flow-wave and floe-floe interaction could be modeled as a wave scattering process (Bennetts & Squire 2009), with the flexural dynamics of the individual floes expected to play an important role (Meylan 2002; Kohout & Meylan 2008; Wadhams 1973). In the case of pancakes, that have diameter $30 \div 100$ cm and thickness $10 \div 30$ cm, scattering and elastic properties are not expected to play an important role. Rather, viscous forces from the grease ice and collisions should dominate.

The scale separation between pancakes and ocean waves suggests the possibility of adapting ideas from suspension theory, treating the individual pancakes as microscopic objects. We are going to model the pancakes as a monodisperse two-dimensional suspension of non-interacting thin disks embedded in a viscous layer that lies on top of an inviscid fluid column. The stress modifications at the water surface will be determined as an average effect from the flow perturbation by the individual pancakes. At macroscopic scale, this will take the form of modified boundary conditions on the wave field at the water surface, which may be interpreted equivalently as a spatially uniform three-layer model, with the infinitely thin top layer accounting for the effect of the pancakes.

This is a necessary first step in the derivation of more elaborate theories valid in the close packing regime characteristic of real pancake ice, in which pancake interactions are taken into account. Some qualitative considerations on the nature and the effect of such interactions will nevertheless be presented and the effect on the wave dispersion discussed.

This paper is organized as follows. In Sec. 2, the flow perturbation by the wave field around an isolated disk will be considered. In Sec. 3, a coarse graining operation will be carried out to evaluate the average stress generated locally in the wave field. In Sec. 4, the resulting modification to the dispersion relation will be determined. In Sec. 5, some qualitative considerations on the close-packing limit will be presented. Sections 6 and 7 will be devoted to discussion of the results and conclusions. Calculation details will be confined to the Appendices.

2. Flow perturbation by a single disk

Consider a random distribution of disks of radius R and thickness $\delta \ll R$, floating on top of an infinitely deep column of fluid of viscosity ν and density ρ . We postpone analysis of the case in which only the top part of the column is viscous to Sec. 3.1. We assume that a small amplitude gravity wave of frequency ω is propagating in the fluid. We want to determine the response of the disks to the wave field in the dilute limit, in which no interaction between the disks are present.

The problem is characterized by two relevant space scales. One is the wavenumber in the case of an infinitely deep inviscid fluid (without the disks), $k_\infty = \omega^2/g$, with $g \simeq 9.8$ m²/s the gravitational acceleration. The other is the thickness of the viscous boundary layer at the water surface,

$$\lambda_\alpha = (\nu/\omega)^{1/2}, \quad (2.1)$$

that is the momentum diffusion length in a wave period. For waves of unperturbed wavelength ≈ 100 m, we would have $\omega \approx 1$ Hz. A typical estimate for the grease ice viscosity is $\nu \approx 0.01$ m²/s (Newyear & Martin 1999; Wadhams et Al. 2004). This would produce a boundary layer of thickness $\lambda_\alpha \approx 0.1$ m. Shorter waves would produce even thinner boundary layers. Smallness of this parameter is an illustration that viscous relaxation is not fast; creeping flow assumptions, characteristic of standard suspension theory, do not apply at the disk scale.

Although the scale separation between λ_α and R is not as clear as that between R and

k_∞^{-1} , we assume the ordering

$$\delta, \lambda_\alpha \ll R \ll k_\infty^{-1} \quad (2.2)$$

and introduce expansion parameters

$$\epsilon_k = k_\infty R \quad \text{and} \quad \epsilon_\alpha = \lambda_\alpha / R. \quad (2.3)$$

Presence of an isolated disk will affect the wave in substantially two ways:

- Possible relative motion of the disk with respect to the fluid.
- Fluid stress at the disk surface due to the rigid structure of the body.

The first is basically an added mass effect, which will be shown to be negligible in the discussion that follows (see end of Sec. 2.2). To evaluate the second effect, we must calculate the flow perturbation generated by presence of the disk in the wave field.

Let us put our reference frame with origin at the disk centre, with the z -axis pointing upward and the x -axis in the direction of propagation of the wave. The velocity field in the absence of the disk would be locally, at the unperturbed water surface $z = 0$:

$$\mathbf{U}(\mathbf{x}, t) = \mathbf{U}(0, t) - 2a(x/R)\mathbf{e}_x - 2[a'(x/R) + c(x/R)^2]\mathbf{e}_z. \quad (2.4)$$

Compatible with the assumption $\epsilon_k \ll 1$, we stop the Taylor expansion for \mathbf{U} at the lowest order necessary to account for tangential and normal stresses on the surface. These stresses are associated with the rigid nature of the body, which imposes no-slip and impermeability boundary conditions. For $\delta \ll R$, these conditions need to be enforced only on the bottom surface of the disk. The velocity perturbation $\mathbf{u}(\mathbf{x}, t)$ will then have to satisfy boundary conditions, at $r = \sqrt{x^2 + y^2} < R$:

$$\mathbf{u}(\mathbf{x}, t) = 2a(x/R)\mathbf{e}_x + [b + 2c(x/R)^2]\mathbf{e}_z, \quad z = 0. \quad (2.5)$$

Notice the presence of the term $b\mathbf{e}_z$ in the perturbation, accounting for possible relative motions of the disk with respect to the fluid. This entails an additional boundary condition to the problem, that is zero total vertical force on the disk, consistent with the assumption $\delta \ll R$ and therefore negligible disk inertia. Notice also absence of a contributions proportional to a' in \mathbf{u} (the disk thus rotates with the unperturbed flow). Again, this is a consequence of the assumption $\delta \ll R$, and therefore negligible moment of inertia of the body.

It is convenient to shift to cylindrical coordinates and express the velocity as a sum over angular harmonics

$$\mathbf{u}(\mathbf{x}, t) = \sum_m \mathbf{u}_m(r, z; t) e^{im\phi}. \quad (2.6)$$

The boundary condition for $r < R$, Eq. (2.5), will thus read

$$\begin{aligned} \mathbf{u}_0(r, 0) &= a(r/R)\mathbf{e}_r + [b + c(r/R)^2]\mathbf{e}_z; \\ \mathbf{u}_{\pm 2}(r, 0) &= (1/2) \left[a(r/R)\mathbf{e}_r \pm ia(r/R)\mathbf{e}_\phi + c(r/R)^2\mathbf{e}_z \right]. \end{aligned} \quad (2.7)$$

For $r > R$, we have to impose zero stress at the free water surface. We have for the tangential stress:

$$\tau_{z\phi} = \mu(\partial_z u_r + \partial_r u_z) = 0, \quad \tau_{zr} = \mu(\partial_z u_\phi + \frac{1}{r}\partial_\phi u_z) = 0, \quad (2.8)$$

and for the normal stress

$$\tau_{zz} = 2\mu\partial_z u_z - P = 0, \quad (2.9)$$

with P the pressure perturbation at the surface and $\mu = \rho\nu$ the dynamic viscosity of the fluid.

The velocity perturbation \mathbf{u} obeys, for small-amplitude waves, the time-dependent Stokes equation

$$\partial_t \mathbf{u} + \rho^{-1} \nabla(P + V) = \nu \nabla^2 \mathbf{u}, \quad \nabla \cdot \mathbf{u} = 0, \quad (2.10)$$

where $V = -\rho g z$ is the gravitational potential. We can express \mathbf{u} in terms of scalar and vector potentials

$$\mathbf{u} = -\nabla \Phi + \nabla \times \mathbf{A}. \quad (2.11)$$

In angular components:

$$\begin{aligned} \mathbf{u}_m = & \left(-\partial_r \Phi_m + \frac{im}{r} A_{m,z} - \partial_z A_{m,\phi} \right) \mathbf{e}_r \\ & + \left(-\frac{im}{r} \Phi_m + \partial_z A_{m,r} - \partial_r A_{m,z} \right) \mathbf{e}_\phi \\ & + \left(-\partial_z \Phi_m + \partial_r A_{m,\phi} + \frac{1}{r} (A_{m,\phi} - im A_{m,r}) \right) \mathbf{e}_z. \end{aligned} \quad (2.12)$$

Notice that for $m = 0$ we can take $\mathbf{A}_0 = A_0 \mathbf{e}_\phi$ (the flow component for $m = 0$ is in essence two-dimensional).

The scalar and vector potentials Φ and \mathbf{A} can be taken to obey, from Eq. (2.10) (see Appendix A)

$$\rho \partial_t \Phi = P + V, \quad \nabla^2 \Phi = 0 \quad (2.13)$$

and

$$\partial_t \mathbf{A} = \nu \nabla^2 \mathbf{A}, \quad \nabla \cdot \mathbf{A} = 0. \quad (2.14)$$

The first of Eq. (2.13) can be used to rewrite the condition of zero normal stress at $r > R$, Eq. (2.9), in the form

$$2\nu \partial_z u_z - g\eta - \partial_t \Phi = 0, \quad (2.15)$$

with η the vertical displacement of the water surface induced by \mathbf{u} , which obeys the equation

$$\dot{\eta}(r, \phi; t) = u_z(r, \phi, 0; t). \quad (2.16)$$

The system of equations formed by the second of Eq. (2.13) and (2.14), with the definition Eq. (2.11) and the boundary conditions Eqs. (2.8) and (2.15), will describe the dynamics of the flow perturbation induced by the disk. For $\nu \rightarrow 0$ it would describe the flow produced by a radius R membrane whose surface oscillates vertically with the law $u_z(\mathbf{x}, t) = b + 2c(x/R)^2$. For $k_\infty R \rightarrow 0$, the effect would be that of a point force quadrupole. Inclusion of viscosity induces local dissipation, which we shall evaluate perturbatively in the limit of small ϵ_α and ϵ_k .

2.1. Boundary layer structure

The small ϵ_α limit is associated to a viscous boundary layer asymptotically thin on the scale of the disk. This suggests a multiscale approach to calculate the vector potential

$$\mathbf{A}(\mathbf{x}) = \mathbf{A}_+(\mathbf{x}) e^{\alpha z}, \quad (2.17)$$

with

$$\alpha = (-i\omega/\nu)^{1/2}, \quad (2.18)$$

and \mathbf{A}_+ slowly dependent on z . We set up the perturbation expansion

$$\Phi = \sum_{n=0}^{\infty} \Phi^{(n)} \epsilon_\alpha^n, \quad \mathbf{A} = \sum_{n=1}^{\infty} \mathbf{A}^{(n)} \epsilon_\alpha^n, \quad (2.19)$$

and use Eq. (2.12) to write the boundary conditions (2.8) and (2.15) in terms of potentials. For $\epsilon_\alpha \ll 1$, we expect distinct behaviours of \mathbf{A} for $r < R$ and $r > R$, separated by a transition region of thickness $\lambda_\alpha \ll R$ (not so for Φ , that is expected to vary on scale k_∞^{-1} everywhere). Keeping only leading order terms, we have in the inner region $r < R$, from Eq. (2.12):

$$\begin{aligned} \partial_z \Phi_m^{(0)} &= -u_{m,z}, & \bar{\alpha} A_{m,\phi}^{(1)} &= -u_{m,r} - \partial_r \Phi_m^{(0)}, \\ \bar{\alpha} A_{m,r}^{(1)} &= u_{m,\phi} + \frac{im}{r} \Phi_m^{(0)}, & \bar{\alpha} &= \alpha/\epsilon_\alpha. \end{aligned} \quad (2.20)$$

The zero divergence condition for \mathbf{A} becomes, for $r < R$:

$$A_{m,z}^{(1)} = 0; \quad \frac{im}{r} A_{m,\phi}^{(1)} + \partial_r A_{m,r}^{(1)} + \frac{1}{r} A_{m,r}^{(1)} + \bar{\alpha} A_{m,z}^{(2)} = 0. \quad (2.21)$$

In the outer region $r > R$, we get instead, from Eqs. (2.8) and (2.15), $A_{m,r}^{(1)} = A_{m,\phi}^{(1)} = 0$, which gives to leading order:

$$\begin{aligned} -\partial_r \partial_z \Phi_m^{(0)} + \frac{im\bar{\alpha}}{r} A_{m,z}^{(1)} - \bar{\alpha}^2 A_{m,\phi}^{(2)} &= 0, \\ -\frac{2im}{r} \partial_z \Phi_m^{(0)} - \bar{\alpha} \partial_r A_{m,z}^{(1)} + \bar{\alpha}^2 A_{m,r}^{(2)} &= 0, \\ V_m^{(0)}/\rho - \partial_t \Phi_m^{(0)} &= 0 \end{aligned} \quad (2.22)$$

(it is easy to see that $\nu \partial_z u_z / \partial_t \Phi = O(\epsilon_\alpha^2)$, while V_m and $\partial_t \Phi$ are of the same order in ϵ_α). The zero divergence condition for \mathbf{A} becomes, for $r > R$:

$$A_{m,z}^{(1)} = 0; \quad \frac{im}{r} A_{m,\phi}^{(2)} + \partial_r A_{m,r}^{(2)} + \frac{1}{r} A_{m,r}^{(2)} + \bar{\alpha} A_{m,z}^{(3)} = 0. \quad (2.23)$$

Putting together Eqs. (2.20) to (2.23), we get to lowest order in ϵ_α the boundary conditions at $z = 0$:

$$\begin{aligned} \partial_z \Phi_m &= -u_{m,z}, & \alpha A_{m,\phi} &= -u_{m,r} - \partial_r \Phi_m, \\ \alpha A_{m,r} &= u_{m,\phi} + \frac{im}{r} \Phi_m, & & r < R, \end{aligned} \quad (2.24)$$

and

$$A_{m,\phi} = A_{m,r} = 0, \quad V_m/\rho - \partial_t \Phi_m = 0, \quad r > R, \quad (2.25)$$

where $\Phi \simeq \Phi^{(0)}$, $\mathbf{A} \simeq \mathbf{A}^{(1)} \epsilon_\alpha$ and $A^{(1)} = (A_r^{(1)}, A_\phi^{(1)}, 0)$. Notice that the divergenceless condition Eq. (2.21) ceases to be necessary (it would provide us with the second order term $A_{m,z}^{(2)}$ that we do not need at the order considered). Similarly for the zero tangential stress conditions at $r > R$.

2.2. Potential component

The potential component of the flow is fully accounted for by the part of the velocity field due to the scalar potential Φ . This obeys the Laplace equation $\nabla^2 \Phi = 0$, with the boundary conditions established by the first of Eq. (2.24) and the second of Eq. (2.25). The boundary condition $V_m/\rho - \partial_t \Phi_m = 0$ in the outer region $r > R$, can be rewritten in terms of potentials using Eqs. (2.15) and (2.16). From Eqs. (2.12) and the first of Eq. (2.25), we have in the external region $r > R$, to lowest order in ϵ_α , $u_z = -\partial_z \Phi$. Putting together with the first of Eq. (2.24), we get the boundary conditions for the scalar potential:

$$\partial_z \Phi = -u_z, \quad r < R,$$

$$\partial_z \Phi - \frac{\omega^2}{g} \Phi = 0, \quad r > R, \quad (2.26)$$

i.e. mixed Neumann and Robin boundary conditions. These must be compounded with the condition of zero vertical force on the disk, required to fix the parameter b in Eq. (2.5). This is

$$\int_{r < R} dS \left[u_z(\mathbf{x}) - \frac{\omega^2}{g} \Phi(\mathbf{x}) \right] = 0, \quad (2.27)$$

where the integral is carried out on the disk surface at $z = 0$.

We solve the boundary value problem defined by Eqs. (2.26) and (2.27) perturbatively in ϵ_k and to lowest order in ϵ_α . We write

$$\Phi = \sum_{n=0}^{\infty} \Phi^{(n)} \epsilon_k^n, \quad (2.28)$$

and similarly for b and \mathbf{u} . It is easy to see that small ϵ_k corresponds to a condition of slow dynamics for the potential component of the flow. This means again that inertia is negligible at the disk scale, which converts the Robin boundary condition at $r > R$ in Eq. (2.26), to lowest order in ϵ_k , to a Neumann boundary condition $\partial_z \Phi^{(0)} = 0$.

We recall the expression for the Neumann Green function for the Laplace equation (see e.g. Jackson 1999):

$$G^N(\mathbf{x}, \hat{\mathbf{x}}) = \frac{1}{|\mathbf{x} - \hat{\mathbf{x}}|} + \frac{1}{|\mathbf{x} - \hat{\mathbf{x}}'|}, \quad \hat{\mathbf{x}}' = (\hat{x}, \hat{y}, -\hat{z}), \quad (2.29)$$

which allows us to write

$$\Phi^{(0)}(\mathbf{x}) = -\frac{1}{2\pi} \int_{r_0 < R} dS_0 \frac{u_z^{(0)}(\mathbf{x}_0)}{|\mathbf{x} - \mathbf{x}_0|}. \quad (2.30)$$

In similar way, the total vertical force in Eq. (2.27) will receive contribution, to lowest order, only from the vertical velocity. In other words, the condition of zero vertical force on the disk coincides with that of zero average vertical component of the velocity perturbation. This gives in Eq. (2.5)

$$b^{(0)} = -c. \quad (2.31)$$

The next orders in the expansion are obtained in iterative fashion from the expression for $\Phi^{(1)}$

$$\begin{aligned} \partial_z \Phi^{(1)} &= -b^{(1)}, & r < R, \\ \partial_z \Phi^{(1)} &= -\frac{1}{R} \Phi^{(0)}, & r > R, \end{aligned} \quad (2.32)$$

where $b^{(1)}$ is obtained from the next order in the condition of zero average normal force, Eq. (2.27):

$$b^{(1)} = \frac{1}{\pi R^2} \int_{r < R} dS \Phi^{(0)}(\mathbf{x}). \quad (2.33)$$

The coefficient $b^{(1)}$ gives the first contribution to the relative vertical motion of the disk with respect to the fluid. No such contribution exists horizontally, due to the linear approximation in Eq. (2.4) for U_x , and to the fact that δ is assumed small. The last condition has the consequence that horizontal pressure differences on the lateral surface are negligible compared to the viscous stresses on the bottom of the disk.

3. The stress perturbation

We want to determine the stress generated on the water surface by the disks. In the dilute limit, this is the sum of the stresses generated by the disks individually, neglecting their mutual interaction. By construction, the only place where the surface stress is non-zero is under a disk. From Eq. (2.12), the stress under a disk will be, working to lowest order in ϵ_k and ϵ_α :

$$\tau_{zr} = \mu \left(\partial_z u_{m,r} + \partial_r u_{m,z} \right) \simeq -\mu \alpha^2 A_{m,\phi}, \quad (3.1a)$$

$$\tau_{z\phi} = \mu \left(\partial_z u_{m,\phi} + \frac{1}{r} \partial_\phi u_{m,z} \right) \simeq \mu \alpha^2 A_{m,r}, \quad (3.1b)$$

$$\tau_{zz} = 2\mu \partial_z u_{m,z} + V_m - \rho \partial_t \Phi \simeq \frac{i\rho g}{\omega} u_{m,z}. \quad (3.1c)$$

We notice that the vector potential in the tangential components can be expressed by means of Eq. (2.24), as a function of the velocity \mathbf{u} and of derivatives of the scalar potential Φ . Thus, the only field whose spatial structure we actually need to know is the scalar potential Φ .

At a macroscopic scale, the cumulative effects of the disks is evaluated by means of a local spatial average, which is carried out summing over all the possible positions of a disk, relative to a hypothetical fixed sensor.

If the disks are distributed randomly, uniformly on the water surface, the only stress components surviving the average will be, by symmetry, the ones along xz and zz . We find from Eqs. (3.1 a,b)

$$\langle \tau_{zx} \rangle = -\frac{f\alpha^2\mu}{\pi R^2} \int_0^{2\pi} d\phi \int_0^R r dr \left[A_\phi \cos \phi + A_r \sin \phi \right], \quad (3.2)$$

while, from Eq. (3.1 c),

$$\langle \tau_{zz} \rangle = \frac{if\rho g}{\pi R^2\omega} \int_0^{2\pi} d\phi \int_0^R r dr u_z, \quad (3.3)$$

with f the surface fraction of the disks, which represents the probability that a disk actually lies over the sensor.

It is clear that the integrals in Eqs. (3.2) and (3.3) can be carried out equivalently in the disk reference frame, summing over the sensor positions. This allows to use the expressions in the previous section for the integrands. Care must be taken, however, of the fact that the expansion in Eq. (2.4) is now carried out with respect to different positions in the wave field.

Let us indicate with $\bar{\mathbf{x}} = (\bar{x}, \bar{y}, 0) = (\bar{r}, \bar{\phi}, 0)$ the position of the disk in the laboratory reference frame, and place the sensor at $\bar{\mathbf{x}} = 0$ (see Fig. 1). In the disk reference frame, the sensor will be at $\mathbf{x} = -\bar{\mathbf{x}}$, with $\mathbf{x} = (r, \phi, 0) = (\bar{r}, \bar{\phi} - \pi, 0)$, and the velocity $\mathbf{U}(\mathbf{x}, t)$ at the sensor position will be related to the corresponding expression in the laboratory frame, $\bar{\mathbf{U}}(0, t)$, by

$$\bar{\mathbf{U}}(0, t) = \mathbf{U}(\mathbf{x}, t) = \bar{\mathbf{U}}(\bar{\mathbf{x}}, t) + x \partial_{\bar{x}} \bar{\mathbf{U}}(\bar{\mathbf{x}}, t) + \frac{1}{2} x^2 \partial_{\bar{x}}^2 \bar{\mathbf{U}}(\bar{\mathbf{x}}, t) + \dots \quad (3.4)$$

This gives us the dependence of the coefficients a and c in Eq. (2.4), on $\mathbf{x} = -\bar{\mathbf{x}}$:

$$\begin{aligned} a(\mathbf{x}, t) &= a(0, t) + \frac{Rx}{2} \partial_{\bar{x}}^2 \bar{U}_x(\bar{\mathbf{x}}, t)|_{\bar{\mathbf{x}}=0} + \dots, \\ c(\mathbf{x}, t) &= c(0, t) + \frac{R^2x}{4} \partial_{\bar{x}}^3 \bar{U}_z(\bar{\mathbf{x}}, t)|_{\bar{\mathbf{x}}=0} - \frac{R^2x^2}{8} \partial_{\bar{x}}^4 \bar{U}_z(\bar{\mathbf{x}}, t)|_{\bar{\mathbf{x}}=0} + \dots, \end{aligned} \quad (3.5)$$

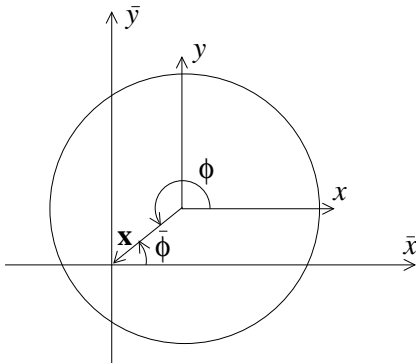


FIGURE 1. Laboratory and floating disk reference frames.

with $a(0, t)$ and $c(0, t)$ the values of a and c when the disk centre is at the sensor position. It is important to notice that neglecting the corrections in Eq. (3.5) would give zero in Eqs. (3.2) and (3.3), as the lowest contribution to the average stress is just the total force on the disk—which is zero, divided by the disk area.

We are now in the position to calculate the average stress. Let us start with the tangential stress. Working to lowest order in ϵ_k and ϵ_α , we have, from Eqs. (3.2), (2.24) and (2.4):

$$\begin{aligned} \langle \tau_{xz} \rangle &= \frac{f\mu\alpha}{\pi R^2} \int_0^{2\pi} d\phi \int_0^R r dr \left[\left(u_r + \partial_r \Phi \right) \cos \phi - \left(u_\phi + \frac{1}{r} \partial_\phi \Phi \right) \sin \phi \right] \\ &= \frac{f\mu\alpha}{\pi R^2} \int_0^{2\pi} d\phi \int_0^R r dr \left[\left(a \frac{r}{R} + \partial_r \Phi_0 \right) \cos \phi \right. \\ &\quad \left. + \left(a \frac{r}{R} + 2\partial_r \Phi_2 \right) \cos 2\phi \cos \phi + \left(a \frac{r}{R} + \frac{4}{r} \Phi_2 \right) \sin 2\phi \sin \phi \right]. \end{aligned} \quad (3.6)$$

Calculations, detailed in Appendix B, allow to write the potential harmonics Φ_0 and Φ_2 in terms of the corresponding harmonics of the Green function G^N in Eq. (2.29). Substituting the expansion in Eq. (3.5) into Eq. (3.6), gives, after some additional algebra:

$$\langle \tau_{xz} \rangle = \frac{11f\mu R^2 \alpha}{64} \frac{\partial^2 \bar{U}_x}{\partial \bar{x}^2} - \frac{Bf\mu\alpha R^3}{2} \frac{\partial^3 \bar{U}_z}{\partial \bar{x}^3}, \quad (3.7)$$

where $B \simeq 0.16$ (see Eq. (B7)). Substituting Eqs. (2.12) and (3.5) into Eq. (3.3), will give in turn

$$\langle \tau_{zz} \rangle = \frac{if\rho g R^4}{64\omega} \frac{\partial^4 \bar{U}_z}{\partial \bar{x}^4}. \quad (3.8)$$

Despite the higher derivatives with respect to \bar{x} in τ_{zz} , the two stress component are of the same order:

$$\frac{\langle \tau_{zz} \rangle}{\langle \tau_{xz} \rangle} \sim \frac{\epsilon_k}{\epsilon_\alpha}. \quad (3.9)$$

On the contrary, the second term to RHS of Eq. (3.7) is smaller than the first by a factor ϵ_k and should be disregarded to the order considered. Thus, to lowest order in ϵ_k and ϵ_α , neither component of the stress depends on the spatial structure of the potential.

3.1. The case of a finite thickness viscous layer

We can extend the analysis to the case in which only a top layer of thickness h of the water column is viscous, and whole basin (including the viscous layer on top) has finite

depth H . We assume

$$H \gg R, \quad k_\infty h \ll 1, \quad (3.10)$$

and take the difference $\rho_w - \rho_i$ between the densities in the inviscid and viscous regions to be small and positive.

Let us consider the modification to the flow perturbation by a single disk. We have seen that to lowest order in $\epsilon_{\alpha,k}$, the normal stress is determined solely by the velocity condition on u_z , and is insensitive to the spatial structure of Φ (see Eq. (3.1)). This means that the only place in which the $\epsilon_k \ll 1$ assumption plays a role remains the Taylor expansion Eqs. (2.4) and (2.5), and the normal stress at the surface remains unaffected by presence of a rigid bottom at $z = -H$.

As regards the tangential part, the main modification to the analysis in Sec. 2 is that the vector potential is confined to the layer $0 > z > -h$ and takes an additional component:

$$\mathbf{A}(\mathbf{x}) = \hat{\mathbf{A}}^+(\mathbf{x})e^{\alpha z} + \hat{\mathbf{A}}^-(\mathbf{x})e^{-\alpha z}. \quad (3.11)$$

The two components are determined imposing simultaneously no-slip under the disks and free-slip at the interface $z = -h$. It is easy to see that the component $\hat{\mathbf{A}}^-$ is exponentially small for $h \gg \lambda_\alpha$. Focusing on the $h \lesssim \lambda_\alpha$ case, we see that the tangential stress at $z = -h$ receives contributions both from the vector and the scalar potential, which are respectively of order $\alpha^2 A$ and Φ/R^2 . In this case, the value of Φ at $z = -h$ will differ from that at $z = 0$ at most by an amount $(h/R)\Phi$. No-slip at $z = 0$ gives, through Eq. (2.24) and (2.25), $\Phi/R \sim \alpha A$, hence, the contribution to tangential stress from Φ is smaller by an amount ϵ_α than that from A . The zero stress condition at $z = -h$ is therefore

$$\hat{A}_{m,r}^+ e^{-\alpha h} + \hat{A}_{m,r}^- e^{\alpha h} = 0 \quad \text{and} \quad \hat{A}_{m,\phi}^+ e^{-\alpha h} + \hat{A}_{m,\phi}^- e^{\alpha h} = 0. \quad (3.12)$$

This gives

$$\hat{\mathbf{A}}^- = -\hat{\mathbf{A}}^+ e^{-2\alpha h} \quad (3.13)$$

which tells us that $\hat{\mathbf{A}}^-$ is exponentially small for $h \gg \lambda_\alpha$. From here we obtain the tangential stress at $z = 0$, exploiting Eq. (2.24):

$$\tau_{zr} = \mu\alpha u_{m,r} \tanh(\hat{\alpha}\psi) \quad \text{and} \quad \tau_{z\phi} = \mu\alpha u_{m,\phi} \tanh(\hat{\alpha}\psi), \quad (3.14)$$

where we have introduced dimensionless quantities

$$\psi = \frac{h}{\lambda_\alpha} = \frac{hk_\infty^{1/4}g^{1/4}}{\nu^{1/2}} \quad \text{and} \quad \hat{\alpha} = \alpha\lambda_\alpha = \sqrt{-i}. \quad (3.15)$$

We arrive at the general expression for the average stress at the surface, working to lowest order in ϵ_k and ϵ_α :

$$\langle \tau_{xz} \rangle = \zeta\alpha\partial_x^2 \bar{U}_x, \quad \langle \tau_{zz} \rangle = \frac{i\sigma}{\omega}\partial_x^4 \bar{U}_z, \quad (3.16)$$

where, from Eqs. (3.7) and (3.8),

$$\zeta = \frac{11f\nu R^2}{64} \tanh(\hat{\alpha}\psi) \quad \text{and} \quad \sigma = \frac{fgR^4}{64}. \quad (3.17)$$

We see that the pancakes act as membrane with a bending rigidity σ and an extensional viscosity $\alpha\zeta$. We note the dependence of σ on an exogenous variable such as g and the complex nature and frequency dependence of ζ , which compound the difficulty in associating a macroscopic viscoelastic behaviour along the line of (Wang & Shen 2010).

4. Dispersion relation

The procedure to derive a dispersion relation for gravity waves in the presence of a viscous layer at the surface is analogous to the one described in (Keller 1998; De Carolis & Desiderio 2002; Wang & Shen 2011). We have to enforce four boundary conditions: continuity of tangential and normal stress at the water surface, $z = 0$; zero tangential stress at the bottom of the viscous layer, $z = -h$; continuity of normal stress again at $z = -h$. Addition of the disks generates non-zero surface stresses, as accounted for by Eqs. (3.16) and (3.17). Imposing continuity between the fluid and the surface stresses gives us:

$$\nu(\partial_x \bar{U}_z + \partial_z \bar{U}_x) = \zeta \alpha \partial_x^2 \bar{U}_x, \quad (4.1a)$$

$$2\nu \partial_z \bar{U}_z - (1/\rho) \bar{P} = \frac{i\sigma}{\omega} \partial_x^4 \bar{U}_z. \quad (4.1b)$$

We write the velocity field of the wave in terms of potentials: $\bar{U}_x = -\partial_x \bar{\Phi} - \partial_z \bar{A}$, $\bar{U}_z = -\partial_z \bar{\Phi} + \partial_x \bar{A}$. In the top viscous layer $-h < z < 0$, we have, from Eq. (2.10):

$$\begin{aligned} \bar{\Phi} &= \bar{\Phi}_+ e^{kz+i(kx-\omega t)} + \bar{\Phi}_- e^{-kz+i(kx-\omega t)}, \\ \bar{A} &= \bar{A}_+ e^{\alpha_k z+i(kx-\omega t)} + \bar{A}_- e^{-\alpha_k z+i(kx-\omega t)}, \end{aligned} \quad (4.2)$$

with $\alpha_k = (-i\omega/\nu + k^2)^{1/2}$. In the inviscid region $-H < z < -h$, only the scalar potential survives:

$$\bar{\Phi} = \bar{\Phi}_w \cosh[k(z+H)] e^{i(kx-\omega t)}, \quad (4.3)$$

where we have enforced the zero vertical velocity condition at the bottom of the column, $z = -H$.

It is convenient to introduce dimensionless quantities

$$\begin{aligned} \hat{k} &= \frac{k}{k_\infty}; & \hat{\nu} &= \frac{k_\infty^{3/2} \nu}{g^{1/2}}; & \hat{\alpha}_k &= \sqrt{-i + \hat{\nu} \hat{k}^2}; & \hat{h} &= k_\infty h; & \hat{H} &= k_\infty H; \\ \hat{\rho} &= \frac{\rho}{\rho_w}; & \xi &= \frac{\epsilon_k}{\epsilon_\alpha} = \frac{k_\infty^{5/4} g^{1/4} R^2}{\nu^{1/2}}; & \hat{\zeta} &= \frac{11\xi f}{64} \tanh(\hat{\alpha}_k \psi); & \hat{\sigma} &= \frac{\xi^2 f}{64}; \end{aligned} \quad (4.4)$$

Dependence on the two small parameters ϵ_k and ϵ_α has been replaced by that on $\hat{\nu} \equiv (\epsilon_k \epsilon_\alpha)^2$ and \hat{h} . Notice that we can write $\hat{h} = \hat{\nu}^{1/2} \psi$ and since ψ is $O(1)$ in most situation of interest, we end up with a single independent small parameter. Notice also that we can write $\hat{\nu} = (k_\infty \lambda_\alpha)^2$, meaning that the natural expansion parameters for the wave dynamics are independent of R . For wavelength ≈ 100 m, an effective viscosity $\nu \approx 0.01$ m²/s and a thickness of the viscous layer $h \approx 0.5$ m, we would have $\psi \approx 4.4$, corresponding to $\hat{\nu} \approx 5 \cdot 10^{-5}$ and $\hat{h} \approx 0.03$. The relevant parameter accounting for the disk radius is now ξ , that in the case of pancake ice tends to be rather small (with the same wave parameters as before, taking $R \approx 0.5$ m would give $\xi \approx 0.14$), but could become larger than one for lower viscosity and shorter waves.

In terms of potentials, the condition of continuity for the tangential stress at the surface, Eq. (4.1 a), becomes

$$\begin{aligned} \hat{\nu} \hat{k}^2 [(2 + \hat{\zeta} \hat{\alpha}_k) \bar{\Phi}_+ + (-2 + \hat{\zeta} \hat{\alpha}_k) \bar{\Phi}_-] - (1 + \hat{\nu}^{1/2} \hat{\zeta} \hat{k}^2 + 2i \hat{\nu} \hat{k}^2) \bar{A}_+ \\ - (1 - \hat{\nu}^{1/2} \hat{\zeta} \hat{k}^2 + 2i \hat{\nu} \hat{k}^2) \bar{A}_- = 0. \end{aligned} \quad (4.5)$$

In similar way, the continuity condition on surface normal stress, Eq. (4.1 b), becomes, using Eqs. (2.13), (2.15) and (2.16) to express pressure in terms of potentials:

$$[\hat{k} - 1 - \hat{\nu} \hat{k}^2 (2i + \hat{\sigma} \hat{k}^3)] \bar{\Phi}_+ + [-\hat{k} - 1 - \hat{\nu} \hat{k}^2 (2i - \hat{\sigma} \hat{k}^3)] \bar{\Phi}_-$$

$$-i\hat{k}(1 - 2i\hat{\nu}^{1/2}\hat{\alpha} - \hat{\nu}\hat{\sigma}\hat{k}^4)\bar{A}_+ - i\hat{k}(1 + 2i\hat{\nu}^{1/2}\hat{\alpha} - \hat{\nu}\hat{\sigma}\hat{k}^4)\bar{A}_- = 0. \quad (4.6)$$

We see that for ξ fixed, sending $\hat{\nu}$ to zero corresponds to sending to zero also the contribution from the disks (the $\hat{\nu} \rightarrow 0$ limit at fixed ξ coincides with an $\epsilon_k \rightarrow 0$ limit at constant ν).

Calculations analogous to those leading to Eqs. (4.5) and (4.6) allow us to write continuity conditions at the interface for the tangential stress:

$$2\hat{\nu}\hat{k}^2(\bar{\Phi}_+e^{-\hat{k}\hat{h}} - \bar{\Phi}_-e^{\hat{k}\hat{h}}) - (1 + 2i\hat{\nu}\hat{k}^2)(\bar{A}_+e^{-\hat{\alpha}_k\psi} + \bar{A}_-e^{\hat{\alpha}_k\psi}) = 0, \quad (4.7)$$

and for the normal stress (see Appendix C):

$$\begin{aligned} & \{i[\hat{\rho} - q_{H-h} + (1 - \hat{\rho})\hat{k}] - 2\hat{\rho}\hat{\nu}\hat{k}^2\}\bar{\Phi}_+e^{-\hat{k}\hat{h}} + \{i[\hat{\rho} + q_{H-h} - (1 - \hat{\rho})\hat{k}] - 2\hat{\rho}\hat{\nu}\hat{k}^2\}\bar{\Phi}_-e^{\hat{k}\hat{h}} \\ & + [(1 - \hat{\rho})\hat{k} - q_{H-h} + 2i\hat{\rho}\hat{\nu}^{1/2}\hat{\alpha}\hat{k}]\bar{A}_+e^{-\hat{\alpha}_k\psi} \\ & + [(1 - \hat{\rho})\hat{k} - q_{H-h} - 2i\hat{\rho}\hat{\nu}^{1/2}\hat{\alpha}\hat{k}]\bar{A}_-e^{\hat{\alpha}_k\psi} = 0, \end{aligned} \quad (4.8)$$

where

$$q_H(\hat{k}) = \frac{1}{\tanh(\hat{k}\hat{H})}. \quad (4.9)$$

We have a system of four equations (4.5), (4.6), (4.7) and (4.8), in the four variables $\bar{\Phi}_\pm$ and \bar{A}_\pm , which, for $\hat{\zeta} = \hat{\sigma} = 0$, reduce to Eqs. (15-18) in (Keller 1998). From here, a dispersion relation can be extracted equating to zero the secular determinant. We proceed perturbatively in $\hat{\nu}^{1/2}$ or equivalently, for ψ not large and fixed, in powers of \hat{h} . We write

$$\hat{k} = \sum_k \hat{k}^{(n)} \hat{h}^n \quad (4.10)$$

and likewise expand the secular determinant

$$S(\hat{k}, \hat{h}) = \left[S + \hat{h}(\hat{k}^{(1)}\partial_{\hat{k}} + \partial_{\hat{h}})S + \dots \right]_{\hat{k}=\hat{k}^{(0)}, \hat{h}=0}. \quad (4.11)$$

The dispersion relation $S(\hat{k}, \hat{h}) = 0$ is solved equating to zero order by order the coefficients in the expansion in Eq. (4.11). The operation is sped-up with the help of a symbolic manipulation program.

Let us focus for the moment on the case of a infinite depth basin $H \rightarrow \infty$, for which $\hat{k}^{(0)} = 1$. Stopping the perturbative expansion at $O(\hat{\nu}^{3/2})$, we obtain

$$\begin{aligned} \hat{k} & \simeq 1 + \hat{\nu}\hat{\rho}[i\hat{\alpha}\hat{\zeta} + \hat{\sigma}] + \hat{\nu}^{3/2}\psi \left\{ 8\hat{\rho} \left[i + \frac{\hat{\alpha} \cosh \hat{\alpha}\psi - 1}{\psi \sinh \hat{\alpha}\psi} \right] \right. \\ & \left. + 2\hat{\rho}(1 - \hat{\rho})\hat{\sigma} + \left[2\hat{\alpha}\hat{\rho}(1 - \hat{\rho}) - \frac{4\hat{\rho} \cosh \hat{\alpha}\psi - 1}{\psi \sinh \hat{\alpha}\psi} \right] i\hat{\zeta} - \frac{\hat{\rho}\hat{\alpha} \cosh \hat{\alpha}\psi}{\psi \sinh \hat{\alpha}\psi} \hat{\zeta}^2 \right\}, \end{aligned} \quad (4.12)$$

which has a number of relevant limit regimes.

4.1. Limit regimes

If the surface fraction of the disks is not too small and the viscous layer is not too thin,

$$\hat{k} \simeq 1 + \hat{\rho}\hat{\nu}[i\hat{\alpha}\hat{\zeta} + \hat{\sigma}], \quad f, \psi, \xi \text{ finite}. \quad (4.13)$$

Writing $i\hat{\alpha} = 2^{-1/2}(1 + i)$, we see that disks produce a frequency-dependent response consisting of both wave damping and decreased wave propagation speed. The viscous layer contributes only a correction at $O(\hat{\nu}^{3/2})$. The information on the layer depth is buried in the dependence on ψ of the tangential stress $\hat{\zeta}$.

The limit of a very thin viscous layer, $h \ll \lambda_\alpha$, which corresponds to putting $\psi \ll 1$ in Eq. (4.12), gives the result, from the first of Eq. (3.17):

$$\hat{k} \simeq 1 + \hat{\rho}\hat{\nu}\hat{\sigma}, \quad \psi \text{ small.} \quad (4.14)$$

Also in this case, the leading contribution comes from the disks.†

The viscous layer will play a role in the absence of disks, i.e. for $f \rightarrow 0$, or when the disks are small, i.e. for $\xi \rightarrow 0$. We get in this case

$$\hat{k} \simeq 1 + 8\hat{\rho}\hat{\nu}^{3/2} \left[i\psi + \hat{\alpha} \frac{\cosh \hat{\alpha}\psi - 1}{\sinh \hat{\alpha}\psi} \right], \quad f \text{ or } \xi \text{ small,} \quad (4.15)$$

which can be brought back to the small \hat{h} deep-water limit of the dispersion relation, Eq. (45) in (Wang & Shen 2010) (see also Keller 1998).

Finally, the limit of an infinitely deep viscous layer could be obtained converting the perturbation expansion in powers of $\hat{\nu}$ at fixed ψ , to one in powers of $\hat{\nu}$ at fixed \hat{h} . The result, stopping at $O(\hat{\nu})$, is

$$\hat{k} \simeq 1 + \hat{\nu} \frac{[4(1 - e^{-2\hat{h}}) + \hat{\alpha}\hat{\zeta}]i + \hat{\sigma}}{1 + (1/\hat{\rho} - 1)e^{-2\hat{h}}}, \quad \hat{h} \text{ finite,} \quad (4.16)$$

which, for large \hat{h} , becomes

$$\hat{k} = 1 + \hat{\nu}[4i + i\hat{\alpha}\hat{\zeta} + \hat{\sigma}], \quad \hat{h} \rightarrow \infty, \quad (4.17)$$

and we recognize, in the disk-free case $f = 0$, the dispersion relation for waves in a viscous fluid derived by Lamb (1932). The transition from a shallow to a deep layer regime occurs in two stages. For $\psi \ll 1$, the disks see the viscous layer as shallow, corresponding to the dispersion relation in Eq. (4.14). They will see the layer as deep for $\psi \gg 1$, which would correspond to setting $\tanh(\hat{\alpha}\psi) = 1$ in the first of Eq. (3.17) and then in Eq. (4.13). Only for $\hat{h} \gg 1$, will Eq. (4.16) converge to the infinite depth solution Eq. (4.17), and will the waves see the viscous layer as deep.

5. Close packing effects

We may try to extend the analysis to real pancake ice conditions, in which the surface fraction f is $O(1)$. In such a regime, the disks will not be free to move horizontally, rather, they will follow neighboring disks. Such an effect could be modeled imagining that the no-slip boundary condition Eqs. (2.5) and (2.7), applies to islands of disks of horizontal size $\sim k^{-1}$, rather than individual disks. This suggests a modification to the expression for the tangential stress in Eqs. (3.16) and (3.17):

$$\tau_{xz} = \frac{c\mu\alpha}{k^2} \partial_x^2 \bar{U}_x \tanh(\hat{\alpha}\psi), \quad (5.1)$$

with c constant. This expression for τ_{xz} is $O(\epsilon_k^{-2})$ larger than the one in the first of Eq. (3.16).

Nothing as dramatic is expected in the normal stress. Pancakes remain free to move vertically and the only modification is expected in the boundary condition for the potential velocity component, Eq. (2.26), that would cease, for $r > R$, to be of zero-stress type.

To allow comparison with pancake ice data from wave tank experiment, we allow

† No dissipation to this order, as the flow perturbation from the disks, in the absence of a viscous layer, becomes purely potential.

$\hat{H} < \infty$. We can repeat the procedure leading to Eq. (4.12) to derive a dispersion relation in the close-packing regime.

Tangential stress balance at the water surface will obey, instead of Eq. (4.5),

$$\begin{aligned} & (c_\psi \hat{\nu}^{1/2} \hat{\alpha} \hat{k} + 2\hat{\nu} \hat{k}^2) \bar{\Phi}_+ + (c_\psi \hat{\nu}^{1/2} \hat{\alpha} \hat{k} - 2\hat{\nu} \hat{k}^2) \bar{\Phi}_- \\ & - (1 + c_\psi + 2i\hat{\nu} \hat{k}^2) \bar{A}_+ - (1 - c_\psi + 2i\hat{\nu} \hat{k}^2) \bar{A}_- = 0, \end{aligned} \quad (5.2)$$

where $c_\psi = c \tanh \hat{\alpha} \psi$. The disks now contribute at $O(\hat{\nu}^{1/2})$ to the dynamics, while before they contributed only at $O(\hat{\nu})$. Notice the limit $c \rightarrow \infty$, that would describe an inextensible disk layer and would lead to zero tangential velocity at the surface (peristaltic flow regime).

Considering a finite depth regime implies that we must now expand around $\hat{k}^{(0)} = \hat{k}_H$, that is the solution to the dispersion relation of gravity waves in a basin of depth H :

$$\hat{k}_H = q_H(\hat{k}_H). \quad (5.3)$$

This means that we must expand in Eq. (4.8)

$$q_{H-h}(\hat{k}) = \hat{k}_H + (\hat{k}_H - \hat{k}^{(1)} \hat{H})(\hat{k}_H^2 - 1) \psi \hat{\nu}^{1/2} + \dots \quad (5.4)$$

Putting to system Eq. (5.2) with Eqs. (4.6) to (4.8), and expanding the resulting secular equation to $O(\hat{\nu}^{1/2})$ gives the dispersion relation

$$\frac{\hat{k}}{\hat{k}_H} \simeq 1 + \hat{\nu}^{1/2} \left\{ \frac{i\hat{\alpha}c\hat{\rho}\hat{k}_H^2 \tanh(\hat{\alpha}\psi)}{(1+c)[1+(\hat{k}_H^2-1)\hat{H}]} + \frac{(1-\hat{\rho})(\hat{k}_H^2-1)\psi}{1+(\hat{k}_H^2-1)\hat{H}} \right\}. \quad (5.5)$$

The second term in braces is the correction that would be produced by an inviscid layer of density different from the rest of the column, which is just a mass-loading effect (recall that $\psi \hat{\nu}^{1/2} = \hat{h}$, which is independent of ν). Pancakes are accounted for by the first term to RHS of Eq. (5.5). The lowest order correction to the ice-free case occurs at $O(\hat{\nu}^{1/2})$, which could be in principle much larger than predicted by straightforward extension of the dilute model (see Eq. (4.12)).

6. Discussion

We study in this Section the dispersion relations derived in Secs. 4 and 5, in situations relevant to real pancake ice.

We consider first the dilute regime described by Eq. (4.12) and its limit forms (4.13) to (4.15). The relation dispersion Eq. (4.12) accounts for the effect of the viscous layer, originally described in the model by Keller (1998), as well as that of the tangential and normal stresses induced by the disks. The two relevant limits, Eq. (4.13) and (4.15), correspond to situations in which the stress by the disks and by the viscous layer, respectively, are dominant. The magnitude of the stress by the viscous layer and by the tangential and normal stress components by the disks can be estimated as

$$O(\epsilon_\alpha^3 \epsilon_k^3), \quad O(\epsilon_\alpha \epsilon_k^3) \quad \text{and} \quad O(\epsilon_k^4), \quad (6.1)$$

respectively. For parameters typical of pancake ice in the ocean ($\nu = 0.01 \text{ m}^2/\text{s}$, R , $h < 1 \text{ m}$ and $k_\infty = 0.06 \text{ m}^{-1}$), we find $\epsilon_\alpha > 0.1$. This means that there is not a clear scale separation between the stress contribution by the viscous layer and the tangential stress of the disks. In fact, contrary to what one could guess assuming $\epsilon_{\alpha,k} \ll 1$ in Eq. (6.1), as shown in Fig. 2, there are situations in which the viscous layer dominates over the effect of the disks. This is more pronounced for damping than for wave dispersion. Inspection of

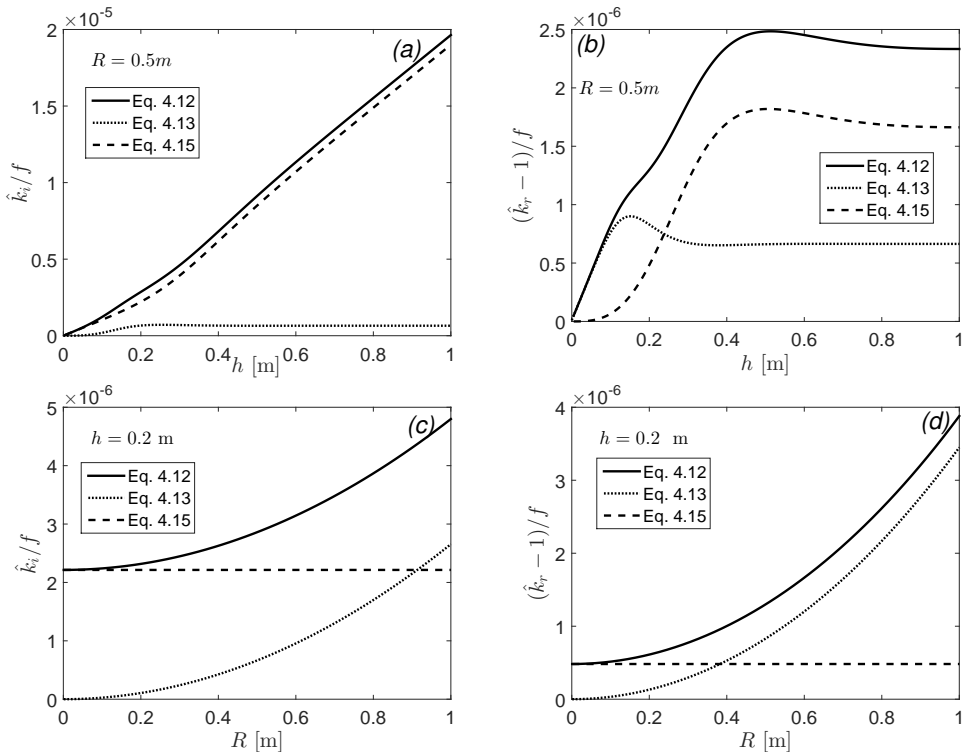


FIGURE 2. Plots of wave damping (panels (a) and (c)), and wave dispersion (panels (b) and (d)), in a typical pancake ice scenario. Values of the parameters: $\nu = 10^{-2} \text{ m}^2/\text{s}$, $k_\infty = 0.06 \text{ m}^{-1}$, $\hat{\rho} = 0.917$, corresponding to $\lambda_\alpha = 0.1142 \text{ m}$ and $\hat{\nu} = 4.69 \cdot 10^{-5}$, and to $\xi = 0.13$ in panels (a) and (b), and $\psi = 1.75$ in panels (c) and (d).

Eq. (4.12) and of its limit forms tells us that the viscous layer's effect is mainly damping of the waves, while the disks produce both damping and dispersion. The damping by the viscous layer turns out to be larger than that by the disks (the origin of this is that ϵ_α is not small enough compared to the numerical coefficients in Eq. (4.12)). This implies that damping dominates over dispersion in most of the parameter range considered, and therefore that the effect of disks on wave damping is small. The effect decreases at larger h and smaller R .

The situation is different as regards wave dispersion, as the viscous layer contribution to $\hat{k}_r - 1$ is much smaller than that to \hat{k}_i . This has the consequence that when the viscous layer is thin enough (less than $\sim \lambda_\alpha$ in thickness), the disks dominate dispersion.

The situation changes drastically when ϵ_k and ϵ_α are both small and $\xi = \epsilon_k/\epsilon_\alpha = O(1)$. Such a condition could be realized, in the range of h and R of Fig. 2, using a smaller viscosity. In the context of pancake ice, examples in which a smaller viscosity could be considered are generally related to the presence of oil: situations include oil spilling under pancake ice and oil incorporated into the ice as grease ice is formed (Fingas 2003). We repeat in Fig. 3 the analysis in Fig. 2 adopting $\nu = 10^{-4} \text{ m}^2/\text{s}$. In this case, we see that wave dispersion is dominated by the disks, while damping is dominated by the disks only for small h and large R . In this parameter range, damping and dispersion are of the same order of magnitude. The slow dependence of the disk stress on h is due to the fact that for small ν , λ_α is small as well, ψ is consequently large, and the tangential stress in Eqs. (3.16) and (3.17) reaches a plateau.

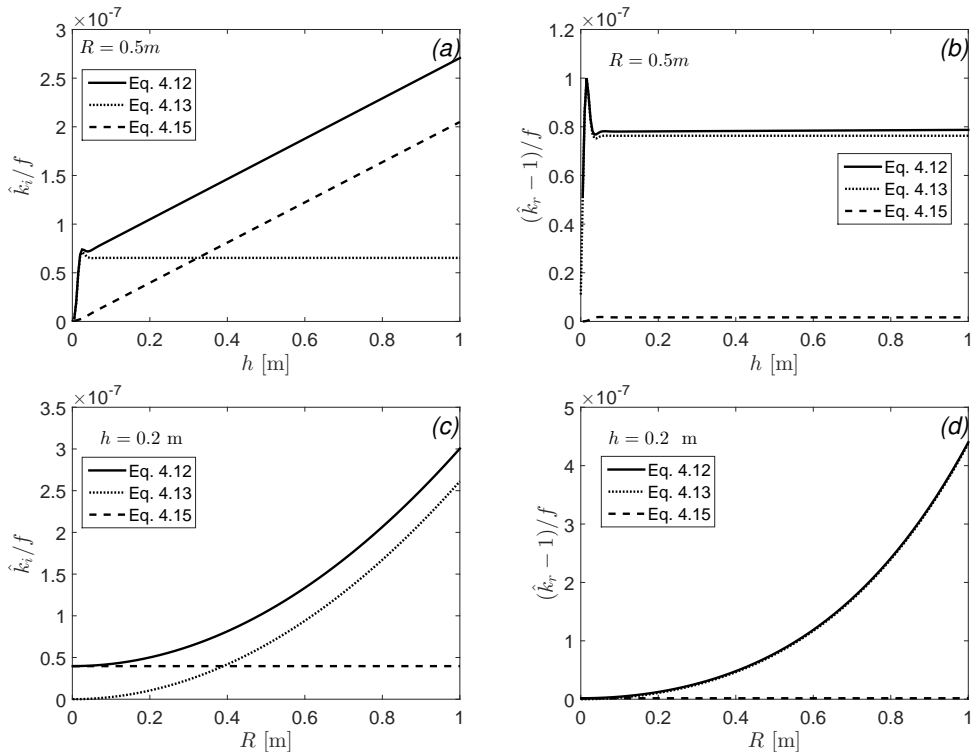


FIGURE 3. Plots of wave damping (panels (a) and (c)), and wave dispersion (panels (b) and (d)), in a possible pancake ice - mixed oil scenario. Values of the parameters: $\nu = 10^{-4} \text{ m}^2/\text{s}$, $k_\infty = 0.06 \text{ m}^{-1}$, $\hat{\rho} = 0.917$, corresponding to $\lambda_\alpha = 0.01 \text{ m}$ and $\hat{\nu} = 4.69 \cdot 10^{-7}$, and to $\xi = 1.3$ in panels (a) and (b), and $\psi = 17.5$ in panels (c) and (d).

Let us shift our consideration to the close packing model of Sec. 5. We have considered a model frazil-pancake ice situation, with pancake radius $R = 0.6 \text{ m}$ and frazil layer thickness $h = 0.5 \text{ m}$.

As expected, for long wavelengths, the close-packing model Eq. (5.5) predicts a wave damping that is orders of magnitude larger than predicted considering a nominally $f = 1$ condition in the dilute model Eq. (4.12) (see Fig. 4a). We recall that in this range, the damping predicted by the dilute model comes mainly from the viscous layer. The results in Fig. 4a have been obtained setting $c = 0.2$ in Eq. (5.5), corresponding to pancake island with diameter of the order of one third of the wavelength. For fixed pancake radius, the number of pancakes in an island will increase with the wavelength (in the range $k_\infty < 0.2 \text{ m}^{-1}$, each pancake island will contain at least eighty pancakes). For shorter wavelengths the approximation $\epsilon_k \ll 1$ at the basis of the derivation of the stress expressions, Eqs. (3.16) and (3.17), and consequently of the dispersion relations Eqs. (4.12) and (5.5), cease to be valid. We can nevertheless try to extrapolate our model to the range $\epsilon_k \lesssim 1$, solving without any perturbation expansion the set of equations (4.5) to (4.8) in the dilute case, and that of Eqs. (5.2) and (4.6) to (4.8) in the close packing case. It should be stressed that in this way we are including only a part of the higher order contributions in ϵ_k to the dispersion relation, as the stresses in Eqs. (3.16) and (3.17) continue to be evaluated to lowest order in that parameter. The two extended dispersion relations tend to coincide at short wavelengths, which is reasonable, since the

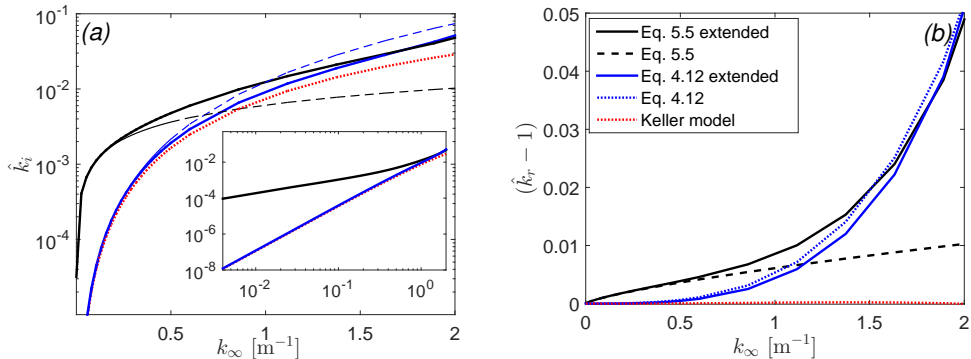


FIGURE 4. Comparison of the predictions by the close packing model, the dilute model and the Keller's model, in a typical pancake ice scenario. Values of the parameters: $\nu = 10^{-2} \text{ m}^2/\text{s}$, $\hat{\rho} = 0.917$, $h = 0.5 \text{ m}$, $R = 0.6 \text{ m}$, $f = 1$ and $c = 0.2$. Panel (a) wave damping; panel (b) dispersion.

number of pancakes in a pancake island will decrease to one in that limit (see solid curves in Fig. 4a).

As regards wave dispersion, as shown in Fig. 4b, both Eqs. (4.12) and (5.5) and their extension to $\epsilon_k \approx 1$, lead to decrease of the wave phase velocity. As in the case of damping, the close packing model gives a result that is orders of magnitude larger than the dilute model at large wavelengths. We have included for reference the prediction of the viscous layer model by Keller (1998). Both in regard to damping and to wave dispersion, we see that the predictions by the Keller model and those by the dilute model become different only for short wavelengths.

We have tried to use the dispersion relations Eqs. (4.12) and (5.5) to fit the data on wave damping in ocean covered by ice floes ($R = 10 \text{ m}$) from (Wadhams et Al. 1988, Bering Sea data 7th of February 1983). We find reasonable agreement between the close-packing model and the field data for values of the parameters $\nu = 0.01 \text{ m}^2/\text{s}$, $h = 0.16 \text{ m}$ and $c = 1.3$. The value of c considered corresponds to pancake islands with diameter of the order of one wavelength. The values of the effective viscosity and of the top layer thickness are compatible with the presence both of a grease ice layer and a turbulent boundary layer generated by the wind stresses. In order for the dilute model Eq. (4.12) to provide wave damping of the same order of magnitude, an effective viscosity in the top layer $\nu \approx 1 \text{ m}^2/\text{s}$ should be utilized, which seems rather unrealistic. Both models fail to predict the evident rollover in the spectrum at $k_\infty > 0.06 \text{ m}^{-1}$.

7. Conclusion

In this paper we have derived a microscopic theory of gravity wave propagation in ocean covered with disk-like impurities embedded in a viscous layer. In order to allow analytical treatment, a dilute regime (low surface fraction of the disks) has been considered first. We have concentrated the analysis on a regime of long wavelengths and small depth of the viscous boundary layer (the parameter λ_α in Eq. (2.1)) compared with the disk radius. This regime may describe the propagation of gravity waves in ocean covered with both grease ice and solid ice in size ranging from that of pancakes to that of small floes (of size much less than a wavelength).

The effect on the wave dynamics has been determined from surface average of the stress by the disks. The resulting behaviour could not be explained in terms of a viscoelastic

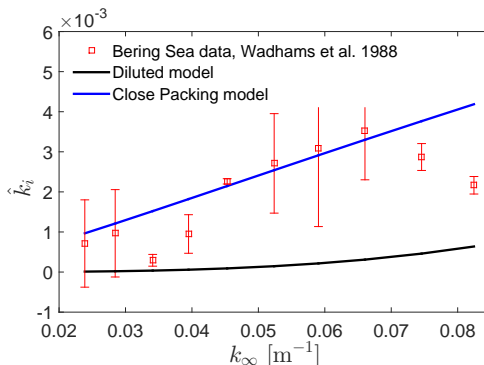


FIGURE 5. Comparison of field data on wave damping by ice floes ($R = 10$ m) (Wadhams et Al. 1988) and prediction by the dilute and close packing models Eqs. (4.12) and (5.5). Values of the parameters $\nu = 0.01 \text{ m}^2/\text{s}$, $h = 0.16$ m $f = 1$ and $c = 1.3$.

constitutive law for the surface layer, as in (Wang & Shen 2010). The normal component of the stress, which is associated with the potential part of the flow perturbation, appears to contribute only to wave dispersion, while the tangential component, which can be interpreted as the result of friction between pancakes and the grease ice layer, produces both damping and dispersion. In most cases of interest, the contribution of the normal stress is negligible.

We have used the dilute limit as an intermediate step to the development of a theory taking into account (at least qualitatively) the interactions between the disks. A simple locking mechanism of the disks into rigid agglomerates with extension of the order of a wavelength has been invoked. The mechanism is linear, which implies that the wave decay remains exponential and is not power-law as predicted e.g. in (Wadhams 1973). Accordingly, we are unable within our approach to give account of any rollover effect, predicted instead by nonlinear models such as the one by Shen and Squire (1998).

For long waves, the locking mechanism produces orders of magnitude increase of both damping and dispersion with respect to artificially setting the surface fraction of the pancakes equal to one in the dilute model. We have compared the predictions by the dilute and the close packing model with field data of wave propagation in ocean covered with ice floes (Wadhams et Al. 1988). Using values of the parameters compatible with presence of a grease ice layer or a turbulent boundary layer (viscosity $\nu = 0.01 \text{ m}^2/\text{s}$, thickness $h = 0.16$ m), we have observed that the data can be better fitted with the close packing than with the dilute model. Fitting with the dilute model, or with a pure viscous model such as the one in (Keller 1998) would require indeed much larger (and difficult to justify) values of the effective viscosity.

A result that stems from the present analysis is the importance of the viscous layer contribution to the disk dynamics also when the layer is very thin. This condition may be of some relevance in the case of large floes, also in light of the possible presence of an eddy viscosity contribution in the dynamics. In the case of large floes, a description in terms of an inviscid theory is usually adopted (Squire et Al. 1995). Our results suggest that viscous effects may be worth being taken into account. Unfortunately, extension of the present theory to a short wave regimes does not seem feasible and the hypothesis remains difficult to verify. Furthermore, we have assumed from the start the disks to have negligible thickness, and the effect on the dynamics of a disk thickness comparable, say, to the depth of the viscous boundary layer, remains to be established.

Acknowledgements

We wish to thank Peter Wadhams for suggestions in the initial phase of the work. This research was supported by FP7 EU project ICE-ARC (Grant agreement No. 603887) and by MIUR-PNRA, PANACEA project (Grant No. 2013/AN2.02).

Appendix A. Potential representation of time-dependent Stokes flows

We decompose the fluid velocity as

$$\mathbf{u} = -\nabla\Phi + \nabla \times \mathbf{A}. \quad (\text{A } 1)$$

Assuming incompressibility, we have that Φ is potential

$$\nabla \cdot \mathbf{u} = 0 \Rightarrow \nabla^2\Phi = 0. \quad (\text{A } 2)$$

The time-dependent Stokes equation is

$$\partial_t \mathbf{u} + \frac{1}{\rho} \nabla P = \nu \nabla^2 \mathbf{u} + \frac{1}{\rho} \mathbf{f}, \quad (\text{A } 3)$$

from which we get the vorticity equation

$$\partial_t [\nabla \times \mathbf{u}] = \nu \nabla^2 [\nabla \times \mathbf{u}] \quad (\text{A } 4)$$

(we consider for simplicity the case in which the force field is of gradient type); in terms of potentials:

$$\partial_t [\nabla \nabla \cdot \mathbf{A} - \nabla^2 \mathbf{A}] = \nu \nabla^2 [\nabla \nabla \cdot \mathbf{A} - \nabla^2 \mathbf{A}], \quad (\text{A } 5)$$

and, if we assume \mathbf{A} divergenceless,

$$\partial_t \nabla^2 \mathbf{A} = \nu \nabla^2 \nabla^2 \mathbf{A}. \quad (\text{A } 6)$$

Equation (A 6) has general solution $\mathbf{A} = \bar{\mathbf{A}} + \mathbf{A}'$, where

$$\partial_t \bar{\mathbf{A}} = \nu \nabla^2 \bar{\mathbf{A}}, \quad \nabla^2 \mathbf{A}' = 0. \quad (\text{A } 7)$$

If we continue to assume that \mathbf{A} is divergenceless, we see that \mathbf{A}' does not contribute to vorticity

$$\nabla \times [\nabla \times \mathbf{A}'] = -\nabla^2 \mathbf{A}' = 0. \quad (\text{A } 8)$$

We could decompose

$$\mathbf{A}' = \nabla q + \nabla \times \mathbf{C}, \quad \nabla^2 q = 0. \quad (\text{A } 9)$$

We have

$$\nabla^2 \mathbf{A}' = \nabla \times \nabla^2 \mathbf{C} = 0 \Rightarrow \nabla^2 \mathbf{C} = \nabla g, \quad (\text{A } 10)$$

which allows us to write the contribution of \mathbf{A}' to the velocity in the form

$$\nabla \times \mathbf{A}' = \nabla (\nabla \cdot \mathbf{C} - g). \quad (\text{A } 11)$$

We see that adding a potential term \mathbf{A}' to the vector potential has the same effect as renormalizing the scalar potential:

$$\Phi \rightarrow \Phi + g - \nabla \cdot \mathbf{C}. \quad (\text{A } 12)$$

In general, the equation for the scalar potential will be

$$-\partial_t \nabla (\Phi + g - \nabla \cdot \mathbf{C}) + \frac{1}{\rho} \nabla P = \frac{1}{\rho} \mathbf{f}. \quad (\text{A } 13)$$

The equation will simplify if $\mathbf{A}' = 0$, i.e. if we assume that \mathbf{A} obeys the first of Eq. (A 7). In this case we shall have, taking $\mathbf{f} = -\nabla V$:

$$\partial_t \Phi = \frac{P+V}{\rho} \quad \text{and} \quad \partial_t \mathbf{A} = \nu \nabla^2 \mathbf{A}, \quad (\text{A } 14)$$

that are Eqs. (2.13) and (2.14).

Appendix B. Green function of the potential component

It is convenient to expand the Neumann Green function, Eq. (2.29), in angular harmonics:

$$G^N(\mathbf{x}, \mathbf{x}_0) = \frac{2}{\sqrt{r^2 + r_0^2}} \sum_m g_m^N \left(\frac{rr_0}{r^2 + r_0^2} \right) e^{im(\phi_0 - \phi'_0)}, \quad (\text{B } 1)$$

with

$$g_m^N(x) = \frac{1}{2\pi} \int_0^{2\pi} d\phi \frac{e^{-im\phi}}{\sqrt{1+x\cos\phi}}. \quad (\text{B } 2)$$

Thus

$$\Phi^{(0)}(\mathbf{x})|_{z=0} = \sum_m \Phi_m^{(0)}(r, 0) e^{im\phi_0}, \quad (\text{B } 3)$$

where

$$\Phi_m^{(0)}(r, 0) = - \int_0^R r_0 dr_0 \frac{u_{m,z}^{(0)}(r_0, 0)}{\sqrt{r^2 + r_0^2}} g_m^N \left(\frac{rr_0}{r^2 + r_0^2} \right), \quad (\text{B } 4)$$

with similar expressions holding at higher orders. This allows to rewrite Eq. (3.6) as

$$\begin{aligned} \langle \pi_{xz} \rangle &\simeq \frac{f\mu\alpha}{2\pi R} \frac{\partial^2 \bar{U}_x}{\partial \bar{x}^2} \int_0^{2\pi} d\phi \int_0^R r^2 dr \left[\frac{r}{2R} (\cos^4 \phi + \sin^2 2\phi) \right] \\ &\quad - \frac{f\mu\alpha}{4\pi} \frac{\partial^3 \bar{U}_z}{\partial \bar{x}^3} \int_0^{2\pi} d\phi \int_0^R r^2 dr \left\{ \cos^2 \phi \right. \\ &\quad \times \partial_r \int_0^R r_0 dr_0 \frac{(r_0/R)^2 - 1}{\sqrt{r^2 + r_0^2}} g_0^N \left(\frac{rr_0}{r^2 + r_0^2} \right) + 2 \left(\cos 2\phi \cos^2 \phi \partial_r \right. \\ &\quad \left. \left. + \frac{\sin^2 2\phi}{r} \right) \int_0^R r_0 dr_0 \frac{(r_0/R)^2 - 1}{\sqrt{r^2 + r_0^2}} g_2^N \left(\frac{rr_0}{r^2 + r_0^2} \right) \right\}. \end{aligned} \quad (\text{B } 5)$$

Carrying out the polar integrals and integrating by part in R where necessary, we find

$$\begin{aligned} \langle \pi_{xz} \rangle &\simeq \frac{11f\mu R^2 \alpha}{64} \frac{\partial^2 \bar{U}_x}{\partial \bar{x}^2} \\ &\quad - \frac{f\mu\alpha}{4} \frac{\partial^3 \bar{U}_z}{\partial \bar{x}^3} \int_0^R r^2 dr \left\{ \partial_r \int_0^R r_0 dr_0 \frac{(r_0/R)^2 - 1}{\sqrt{r^2 + r_0^2}} g_0^N \left(\frac{rr_0}{r^2 + r_0^2} \right) \right. \\ &\quad \left. + \left(\partial_r + \frac{2}{r} \right) \int_0^R r_0 dr_0 \frac{(r_0/R)^2 - 1}{\sqrt{r^2 + r_0^2}} g_2^N \left(\frac{rr_0}{r^2 + r_0^2} \right) \right\} \\ &= \frac{11f\mu R^2 \alpha}{64} \frac{\partial^2 \bar{U}_x}{\partial \bar{x}^2} - \frac{Bf\mu\alpha R^3}{2} \frac{\partial^3 \bar{U}_z}{\partial \bar{x}^3}, \end{aligned} \quad (\text{B } 6)$$

with

$$B = \int_0^1 r dr \int_0^1 r_0 dr_0 \frac{1 - r_0^2}{\sqrt{r^2 + r_0^2}} g_0^N \left(\frac{rr_0}{r^2 + r_0^2} \right) \simeq 0.16. \quad (\text{B } 7)$$

Appendix C. Boundary conditions at the bottom of the viscous layer

The derivation of Eq. (4.7) is straightforward and is omitted. We concentrate on continuity of normal stress. We need first to enforce continuity of the normal velocity:

$$\bar{\Phi}_+ e^{-kh} - \bar{\Phi}_- e^{kh} - i(\bar{A}_+ e^{-\alpha_k h} + \bar{A}_- e^{\alpha_k h}) = \bar{\Phi}_w \sinh[k(H-h)]. \quad (\text{C1})$$

Continuity of normal stress gives

$$2\nu\partial_z \bar{U}_z|_{z=-h^+} - P/\rho = -P_w/\rho. \quad (\text{C2})$$

The first of Eq. (2.13) allows us to write

$$P = \rho\{i\omega(\bar{\Phi}_+ e^{-kh} + \bar{\Phi}_- e^{kh}) - \frac{igk}{\omega}\bar{\Phi}_w \sinh[k(H-h)]\} \quad (\text{C3})$$

and

$$P_w = \rho_w \bar{\Phi}_w \{i\omega \cosh(kH) - \frac{igk}{\omega} \sinh[k(H-h)]\}. \quad (\text{C4})$$

Substituting Eqs. (C3) and (C4) into Eq. (C2), and passing to dimensionless variables, we get

$$\begin{aligned} & \hat{\rho}(i + 2\hat{\nu}\hat{k}^2)(\bar{\Phi}_+ e^{-\hat{k}\hat{h}} + \bar{\Phi}_- e^{\hat{k}\hat{h}}) - 2i\hat{\rho}\hat{\nu}^{1/2}\hat{\alpha}\hat{k}(\bar{A}_+ e^{-\hat{\alpha}_k\psi} - \bar{A}_- e^{\hat{\alpha}_k\psi}) \\ & - i\{q_{H-h} - (1 - \hat{\rho})\hat{k}\}\bar{\Phi}_w \sinh[\hat{H} - \hat{h}] = 0, \end{aligned} \quad (\text{C5})$$

where $q_{H-h} = 1/\tanh[k(H-h)]$. We can eliminate $\bar{\Phi}_w$ using Eq. (C1). Putting together, we obtain

$$\begin{aligned} & \{i[\hat{\rho} - q_{H-h} + (1 - \hat{\rho})\hat{k}] - 2\hat{\rho}\hat{\nu}\hat{k}^2\}\bar{\Phi}_+ e^{-\hat{k}\hat{h}} + \{i[\hat{\rho} + q_{H-h} - (1 - \hat{\rho})\hat{k}] - 2\hat{\rho}\hat{\nu}\hat{k}^2\}\bar{\Phi}_- e^{\hat{k}\hat{h}} \\ & + [(1 - \hat{\rho})\hat{k} - q_{H-h} + 2i\hat{\rho}\hat{\nu}^{1/2}\hat{\alpha}\hat{k}]\bar{A}_+ e^{-\hat{\alpha}_k\psi} \\ & + [(1 - \hat{\rho})\hat{k} - q_{H-h} - 2i\hat{\rho}\hat{\nu}^{1/2}\hat{\alpha}\hat{k}]\bar{A}_- e^{\hat{\alpha}_k\psi} = 0, \end{aligned} \quad (\text{C6})$$

that is Eq. (4.8).

REFERENCES

- BATCHELOR, G. K. 1971 Small-scale variation of convected quantities like temperature in turbulent fluid. part 1. general discussion and the case of small conductivity. *J. Fluid Mech.* **5**, 113–133.
- BROWNELL, C. J. & SU, L. K. 2004 Planar measurements of differential diffusion in turbulent jets. *AIAA Paper 2004-2335*.
- BENNETTS, L. G. & SQUIRE, V. A. 2009 Wave scattering by multiple rows of circular ice floes. *J. Fluid Mech.* **639**, 213–238.
- BREKKE, C. & SOLBERG, A.H. S 2005 Oil spill detection by satellite remote sensing. *Remote Sens. Environ.* **95**, 1–13.
- DAI, M., SHEN, H. H., HOPKINS, M. A. & ACKLEY, S. F. 2004 Wave rafting and the equilibrium pancake ice cover thickness. *J. Geophys. Res.* **109**, C07023.
- DE CAROLIS, G. & DESIDERIO, D. Dispersion and attenuation of gravity waves in ice: a two-layer viscous fluid model with experimental data validation. *Phys. Lett. A*, **305**, 399–412.
- DE CAROLIS, G., OLLA, P. & PIGNAGNOLI, L. 2005 Effective viscosity of grease ice in linearized gravity waves. *J. Fluid Mech.* **535**, 369–381.
- FINGAS, M. F. & HOLLEBONE, B. P. 2003 Review of behaviour of oil in freezing environments. *Marine Pollution Bulletin* **47**(9), 333–340.
- KELLER, J. 1998 Gravity waves on ice-covered waters. *J. Geophys. Res.* **105**, 7663–7669.
- KOHOUT, A. & MEYLAN, M. 2008 An elastic plate model for wave attenuation and ice floe breaking in the marginal ice zone. *J. Geoph* **113**, C09016.
- JACKSON, J.D. 1999 Classical electrodynamics. Wiley.

- LAMB, H. 1932 Hydrodynamics. Dover.
- MARTIN, S. 1981 Frazil ice in rivers and oceans. *Ann. Rev. Fluid Mech.* **13**, 379–397.
- MARTIN, S. & KAUFFMAN, P. 1981 A field and laboratory study of wave damping by grease ice. *J. Glaciol.* **27**, 283–314.
- MEYLAN, M. H. 2002 Wave response of an ice floe of arbitrary geometry. *J. Geophys. Res.* **107**, 5.
- NEWYEAR, K. & MARTIN, S. 1999 Comparison of laboratory data with a viscous two-layer model of wave propagation in grease ice. *J. Geophys. Res.* **104(C4)**, 7837–7840.
- SHEN, H. H. & SQUIRE, V. A. 1998 Wave damping in compact ice fields due to interaction between pancakes. In *Antarctic Sea Ice: physical processes, interactions and variability* (ed. Jeffries, M. O.), pp. 325–342. AGU Antarctic Research Series, vol. 74. Washington, DC: American Geophysical Union.
- SQUIRE, V. A., DUGAN, J. P., WADHAMS, P., ROTTIER, P. J. & LIU, A. K. 1995 Of ocean waves and sea ice. *Ann. Rev. Fluid Mech.* **27**, 115–168.
- WADHAMS, P. 1973 Attenuation of swell by sea ice. *J. Geophys.* **78**, 3552–3563.
- WADHAMS, P., SQUIRE, V. A., GOODMAN, D. J., COWAN, A. M., & MOORE, S. C. 1988 The attenuation rates of ocean waves in the marginal ice zone. *Geophys. Res. Lett.* **93.C6**, 6799–6818.
- WADHAMS, P., PARMIGGIANI, F. F. & DE CAROLIS, G. 2002 The use of SAR to measure ocean wave dispersion in frazil-pancake ice fields. *J. Phys. Oceanogr.* **32**, 1721–1746.
- WADHAMS, P., PARMIGGIANI, F. F., DE CAROLIS, G., DESIDERIO, D. & DOBLE, M. J. 2004 SAR imaging of wave dispersion in Antarctic pancake ice and its use in measuring ice thickness. *Geophys. Res. Lett.* **31**, L15305.
- WANG, R. & SHEN, H. H. 2010 Gravity waves propagating into an ice-covered ocean: a viscoelastic model. *J. Geophys. Res.* **115**, C06024A.
- WANG, R. & SHEN, H. H. 2011 A continuum model for the linear wave propagation in ice-covered oceans: An approximate solution. *Ocean Modelling* **38**, 244–250.
- WEBER, J. 1987 Wave attenuation and wave drift in the marginal ice zone. *J. Phys. Oceanogr.* **17**, 2351–2361.

